Nanotube Phonon Waveguide

C. W. Chang,[1,2,*] D. Okawa,[1] H. Garcia,[1] A. Majumdar,[2,3,4] and A. Zettl[1,2,4,†]

[1]*Department of Physics, University of California at Berkeley, California 94720, USA*

[2]*Center of Integrated Nanomechanical Systems, University of California at Berkeley, California 94720, USA*

[3]*Departments of Mechanical Engineering and Materials Science and Engineering, University of California at Berkeley, California 94720, USA*

[4]*Materials Sciences Division, Lawrence Berkeley National Laboratory, Berkeley, California 94720, USA*

(Received 2 May 2007; published 25 July 2007)

We find that the high thermal conductivity of carbon nanotubes remains intact under severe structural deformations while the corresponding electrical resistance and thermoelectric power show compromised responses. Similar robust thermal transport against bending is found for boron nitride nanotubes. Surprisingly, for both systems the phonon mean free path exceeds the characteristic length of structural ripples induced by bending and approaches the theoretical limit set by the radius of curvature. The robustness of heat conduction in nanotubes refines the ultimate limit that is far beyond the reach of ordinary materials.

DOI: 10.1103/PhysRevLett.99.045901 PACS numbers: 65.80.+n, 62.25.+g, 63.22.+m, 73.63.Bd

The invention of optical fibers that allow photons to carry broadband information over long distances and through an arbitrary path with low loss has shaped the modern information age. Optical fibers are engineered to exhibit wide-band transmission, optical confinement, mechanical flexibility, and extraordinary optical nonlinearity. However, because the characteristic length of phonons at room temperature is less than 10 nm, the counterpart fibers for heat conduction are difficult to fabricate using ordinary materials. On the other hand, carbon nanotubes (CNTs) and boron nitride nanotubes (BNNTs) have been shown to exhibit excellent thermal and mechanical properties. The axial heat conduction of a nanotube is dominated by strongly sp^2-bonded phonons, whereas the off-axis phonons interact via weak van der Waals forces. The large disparity between the strength of the in-plane sp^2 bonding and the van der Waals bonding facilitates high thermal conductivity and phonon confinement in nanotubes. Here we show that phonon transport in nanotubes is superior to the counterpart of photon transmission in optical fibers and approaches the theoretical limit that is inaccessible to other materials.

Multiwalled CNTs with diameters ranging from 10 nm to 33 nm were prepared using conventional arc methods [1]. Multiwalled BNNTs were synthesized using an adaptation of a previously reported method [2], yielding samples with typical outer diameter 30–40 nm and length $\sim 10\ \mu$m. Figure 1 shows the microscale test fixtures fabricated for simultaneously measuring thermal conductivity (κ), electrical resistance (R), and thermopower (S) of individual nanotubes. As detailed elsewhere [3], it consists of two suspended SiN_x pads with integrated Pt film heaters or sensors. In addition, two independent Pt electrodes facilitate electrical measurements of the sample [3]. The test fixture was also made adaptable to transmission electron microscopy (TEM) so that the inner and outer diameters (and structural perfection) of the nanotube under study could be directly and unambiguously determined.

The ends of individual nanotubes were rigidly bonded to the heater/sensor pads by depositing trimethyl cyclopentadienyl platinum ($C_9H_{16}Pt$) on them in a scanning electron microscope (SEM). κ, R, and S were then measured at room temperature with the test fixture still inside the SEM. To mechanically deform the nanotube, a sharpened tungsten tip mounted on a pizeodriven manipulator located inside the SEM was used to displace one of the suspended arms of the test fixture. As shown in the inset of Fig. 1, this allowed bending of the nanotube into various shapes. The position of the tungsten tip was carefully chosen so that it would not perturb the original heat profile and calibration of the test fixture. The thermal conductivity of the nanotube was determined from its measured thermal conduc-

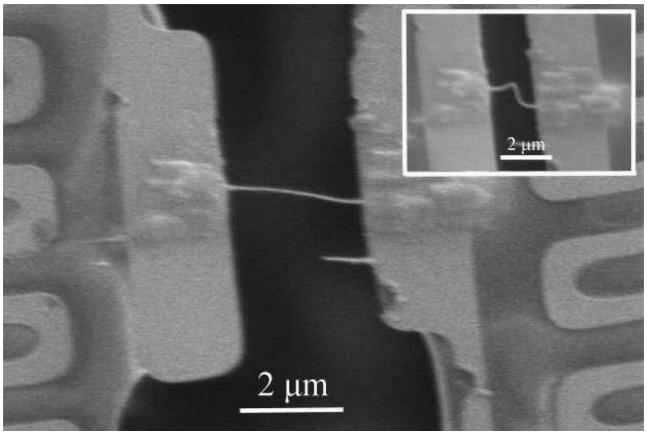

FIG. 1. A SEM image of the microfabricated test fixture with a BNNT spanning the heater/sensor pads (scale bar = 2 μm). Inset. The same BNNT after being bent by moving the pads closer together.

 © 2007 The American Physical Society

tance and the geometrical factors derived from TEM imaging. The phonon mean free path (l) was estimated using $\kappa = Cvl$, where C and v are, respectively, the specific heat [4,5], and the averaged sound velocity ~15 km/s [6].

The upper part of Fig. 2 shows a series of representative SEM images of CNT sample 1 undergoing two cycles of bending. The corresponding changes of R, S, and κ are shown in the lower part of Fig. 2. Values are normalized to the initial quantities of 44 KΩ, −42 μV/K, and 1050 W/m-K, respectively. The electrical resistance shows a cyclic 20% modulation with mechanical deformation. R tracks closely the bending angle, and exhibits maxima where the bending angle is largest, at frames 7 and 15. The increase in R is suggestive of band-gap opening under deformation. Since the total conductance of a multiwalled CNT is dominated by the metallic channels, Fig. 2(a) is consistent with a metal to semiconducting transition when severely bending a metallic tube, a result in accord with previous experiments [7]. It is also consistent with theoretical predictions that indicate a band-gap opening when bending a metallic CNT [8].

The total thermopower S_{total} of a multiwall CNT can be expressed by a two-band model

$$S_{\text{total}} = \frac{\sigma_{\text{metal}} S_{\text{metal}}}{\sigma_{\text{metal}} + \sigma_{\text{semi}}} + \frac{\sigma_{\text{semi}} S_{\text{semi}}}{\sigma_{\text{metal}} + \sigma_{\text{semi}}}, \qquad (1)$$

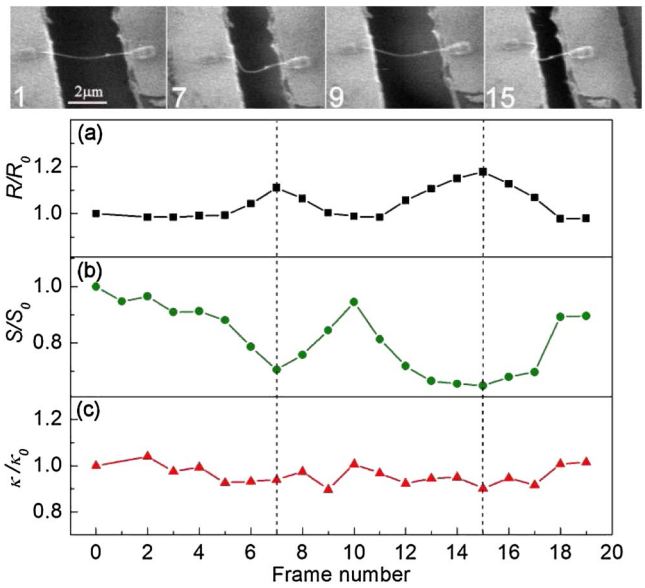

FIG. 2 (color online). Upper: A series of representative SEM images of CNT sample 1 undergoing two cycles of bending (scale bar = 2 μm). The number in each frame denotes the time frame number (time difference between sequent frames ~2 min). Lower: (a) shows the resistance change, (b) shows the thermopower change, and (c) shows the thermal conductivity change while bending the CNT. Their values are normalized to the initial quantities of 44 KΩ, −42 μV/K, and 1050 W/m-K, respectively. The dash vertical lines at frame numbers 7 and 15 identify maximum deformations (the frame numbers correspond to those of the upper SEM images series).

where σ_{metal} and σ_{semi} are electrical conductance of the metallic and semiconducting channels, respectively. S_{metal} and S_{semi} denote the thermopower of the metallic and semiconducting channel, respectively. Although S_{metal} is 1 order of magnitude smaller than S_{semi}, the contribution to S_{total} from the first term in Eq. (1) is largely enhanced by σ_{metal}, which can be more than 3 orders of magnitudes larger than σ_{semi}. Thus the change of S_{total} largely reflects the change in σ_{metal}. As Eq. (1) suggests, a band-gap opening will decrease σ_{metal}, resulting in a decrease of $|S_{\text{total}}|$. Previous experiments have shown that the thermopower of CNTs is sensitive to oxygen absorption, molecular collisions, and gate voltages [9–12]; here we show that it is also sensitive to mechanical deformation.

In contrast, although the thermal conductivity shows a 10% fluctuation as a function of deformation in Fig. 2(c), there is no clear correlation between the thermal conductivity and the bending angles. Especially revealing is the behavior of κ at the deformation extremes (frames 7 and 15) where the bending angles (determined by the projective SEM images) are larger than 90° and 130°, respectively. Since the nanotubes generally move perpendicular to the projective direction (as clearly seen in the 15th frame of Fig. 2 and also in the 13th frame of Fig. 3) and the height difference between the heater and sensor pads is smaller than 50 nm, the real bending angles are undoubtedly larger than the projective angles. The (relatively small) uncorrelated thermal conductivity fluctuations may be due to perturbations in the contacts under large strain. Applying the Wiedemann-Franz law to the data of Fig. 2(a) and comparing the result to Fig. 2(c), we estimate that the electronic contribution to the total thermal conductivity for multiwall carbon nanotubes is less than 1%. The result is consistent with previous theoretical and experimental results for CNTs [13–16].

Figure 3 shows two CNTs under cyclic deformation. The thermal conductivity is normalized to the initial values of 290 W/m-K and 305 W/m-K for CNT samples 2 and sample 3, respectively. At the extremes, the CNTs are bent at angles larger than 125° and 140°, respectively. Unlike Fig. 2, here the two CNTs are buckled locally yielding very small radii of curvature (~70 and ~90 nm, for CNT samples 2 and 3, respectively). Remarkably, κ remains unchanged when the radius of curvature of the deformed nanotube is comparable to the phonon mean free path (~50 nm). Only after extraordinary and permanent mechanical damage to the nanotube, as shown in the last data point of CNT sample 3 where the outer shells of the CNT have been purposely destroyed (inset of Fig. 3), is there a notable decrease in the thermal conductivity value.

To investigate if the robustness of the thermal conductivity of CNTs is specific to that material, or a more general nanotube characteristic, we have extended our study to BNNTs. BNNTs are known to have comparable Young's modulus, phonon dispersion relation and thermal conductivity to CNTs, but because of their large band gap, their thermal properties are purely phononic [4]. As shown in

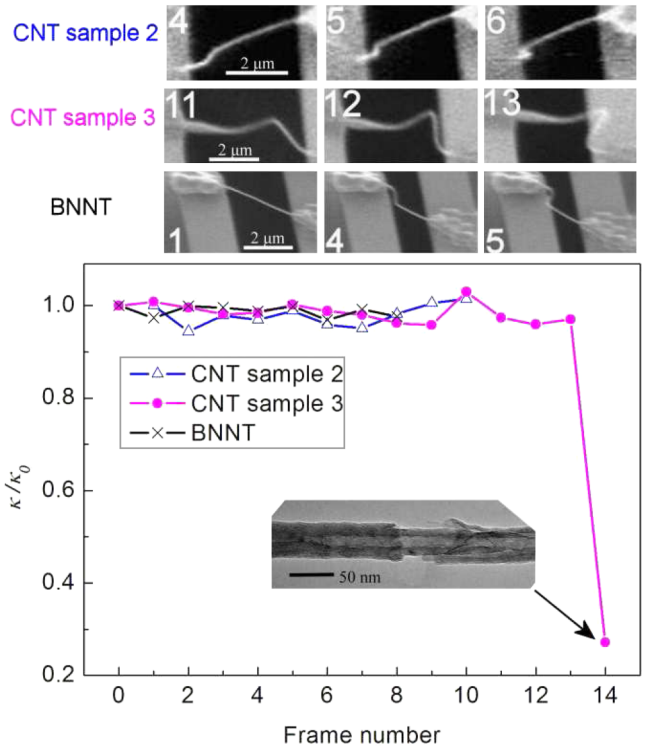

FIG. 3 (color online). Series of representative SEM images of CNT sample 2, CNT sample 3, and a BNNT undergoing cycles of bending. The number in each frame corresponds to the frame number in the lower panel (time difference between sequent frames ~2 min). Lower panel: Normalized thermal conductivity of CNT sample 2 (open triangles), CNT sample 3 (solid circles), and a BNNT (crosses) undergoing cycles of bending. The inset shows a TEM image of CNT sample 3 after the outer walls were compromised, leading to a dramatic decrease in the thermal conductivity (scale bar = 50 nm).

Fig. 3, we have also found that, like CNTs, the thermal conductivity of BNNTs is insensitive to large mechanical bending angles.

We can correlate the change of resistance or thermopower with the band gap modulation in CNTs, but the robustness of the thermal conductivity in CNTs and BNNTs is unexpected. Most materials under strain will sustain defects or dislocations that can effectively scatter phonons and reduce the associated thermal conductivity. Here we find that CNTs or BNNTs do not exhibit mechanical failures or any loss in phonon transport even when bent at an angle larger than 140°.

A ripplelike structure has been observed when bending a multiwalled CNT [17]. Generally, the characteristic wavelength of the ripple is 10 nm for a radius of curvature of ~400 nm and it decreases with increasing bending angle. From a traditional point of view, the phonon mean free path should be limited by the characteristic length of the ripple structures. With a phonon mean free path ~200 nm and a characteristic length of ripples less than 10 nm in CNT sample 1, one might expect the ripples to scatter phonons. Apparently, and somewhat surprisingly, such ripples are ineffective in quenching phonon conduction.

The unusual robustness of phonon transport begs the question of the ultimate limit of phonon transport in nanotubes. Because bending an object also incoherently deflects the path of phonon propagation, bending can create additional phonon scattering even if no defects or dislocations are present. Theoretically, the thermal conductivity of an object will start to decrease when its radius of curvature is smaller than the phonon mean free path. Therefore, the phonon mean free path sets an ultimate limit to the maximum bending curvature beyond which any robustness of phonon transport should no longer hold. We exam this limit for CNT and BNNT samples and find that the robustness of phonon transports of CNTs or BNNTs does not violate, though it is close to, this ultimate limit.

The formation of ripples reduces the effective Young's modulus, and thus decreases the sound velocity [17–19]. Naively, according to $\kappa = Cvl$, a reduction of the sound velocity and phonon mean free path would lead to a large decrease of κ when nanotubes are deformed. The failure of the above analyses suggests that models based on linear approximation cannot be applied for nanotubes.

Recently, the observation of thermal rectification by engineering the mass distribution along a nanotube suggests the presence of lattice solitons [20]. Since solitons are solutions of nonlinear equations and have topological nature, generally it is believed that they are robust against perturbation. Rigorous calculations have confirmed that lattice solitons are insensitive to structural perturbation [21,22]. Thus lattice soliton model explains the unusual robustness of thermal transport observed in this experiment. Because solitons become unstable if the structural perturbations are smaller than its size, from the structural ripples and the minimum radius of curvature set by the present experiment, we determine the soliton size to be less than 10 nm.

For an ordinary microwave waveguide, a slight mechanical deformation will create mismatching of electromagnetic modes, resulting in a significant power loss [23]. When bending an optical fiber, the minimum radius of curvature before optical loss is set by the relative refraction index or the mechanical strength, and is at least 3 orders of magnitude larger than the wavelength of light [23]. Here we show that the phonon mean free path of nanotubes can exceed the characteristic length of the structural ripples and approach the theoretical limit set by the radius of curvature. Therefore, nanotubes not only serve as sensitive nanoelectromechanical devices, but also are excellent and robust phonon waveguides.

This work was supported in part by the Director, Office of Energy Research, Office of Basic Energy Sciences, Division of Materials Sciences, of the U. S. Department of Energy under Contract No. DE-AC03-7600098, and by the NSF within the Center of Integrated Nanomechanical Systems.

*chihwei@berkeley.edu
†azettl@berkeley.edu

[1] D. T. Colbert, J. Zhang, S. M. McClure, P. Nikolaev, Z. Chen, J. H. Hafner, D. W. Owens, P. G. Kotula, C. B. Carter, J. H. Weaver, A. G. Rinzler, and R. E. Smalley, Science **266**, 1218 (1994).
[2] C. Tang, Y. Bando, T. Sato, and K. Kurashima, Chem. Commun. (Cambridge), 1290 (2002).
[3] L. Shi, D. Y. Li, C. H. Yu, W. Y. Jang, D. Kim, Z. Yao, P. Kim, and A. Majumdar, J. Heat Transfer **125**, 881 (2003).
[4] J. Hone, B. Batlogg, Z. Benes, A. T. Johnson, and J. E. Fischer, Science **289**, 1730 (2000).
[5] W. Yi, L. Lu, D. L. Zhang, Z. W. Pan, and S. S. Xie, Phys. Rev. B **59**, R9015 (1999).
[6] M. A. Osman, and D. Srivastava, Phys. Rev. B **72**, 125413 (2005).
[7] S. Paulson, M. R. Falvo, N. Snider, A. Helser, T. Hudson, A. Seeger, R. M. Taylor, R. Superfine, and S. Washburn, Appl. Phys. Lett. **75**, 2936 (1999).
[8] B. Shan, G. W. Lakatos, S. Peng, and K. J. Cho, Appl. Phys. Lett. **87**, 173109 (2005).
[9] K. Bradley, S. H. Jhi, P. G. Collins, J. Hone, M. L. Cohen, S. G. Louie, and A. Zettl, Phys. Rev. Lett. **85**, 4361 (2000).
[10] M. C. Llaguno, J. E. Fischer, A. T. Johnson, and J. Hone, Nano Lett. **4**, 45 (2004).
[11] H. E. Romero, K. Bolton, A. Rosen, and P. C. Eklund, Science **307**, 89 (2005).
[12] J. P. Small, K. M. Perez, and P. Kim, Phys. Rev. Lett. **91**, 256801 (2003).
[13] S. Berber, Y. K. Kwon, and D. Tomanek, Phys. Rev. Lett. **84**, 4613 (2000).
[14] C. W. Chang, A. M. Fennimore, A. Afanasiev, D. Okawa, T. Ikuno, H. Garcia, D. Y. Li, A. Majumdar, and A. Zettl, Phys. Rev. Lett. **97**, 085901 (2006).
[15] C. W. Chang, W. Q. Han, and A. Zettl, Appl. Phys. Lett. **86**, 173102 (2005).
[16] J. Hone, M. Whitney, C. Piskoti, and A. Zettl, Phys. Rev. B **59**, R2514 (1999).
[17] P. Poncharal, Z. L. Wang, D. Ugarte, and W. A. de Heer, Science **283**, 1513 (1999).
[18] T. C. Chang, and J. Hou, J. Appl. Phys. **100**, 114327 (2006).
[19] J. Z. Liu, Q. S. Zheng, and Q. Jiang, Phys. Rev. Lett. **86**, 4843 (2001).
[20] C. W. Chang, D. Okawa, A. Majumdar, and A. Zettl, Science **314**, 1121 (2006).
[21] T. Iizuka and M. Wadati, J. Phys. Soc. Jpn. **62**, 1932 (1993).
[22] T. Iizuka and M. Wadati, J. Phys. Soc. Jpn. **61**, 4344 (1992).
[23] Q. Wang, G. Farrell, T. Freir, G. Rajan, and P. F. Wang, Opt. Lett. **31**, 1785 (2006).